CH_3Cl Dissociation, CH_3 Abstraction, and Cl Adsorption from the Dissociative Scattering of Supersonic CH_3Cl on Cu(111) and Cu(410)

Takamasa Makino[1], Yasutaka Tsuda[2], Akitaka Yoshigoe[2],
Wilson Agerico Diño[3], Michio Okada[1,4]

[1]Department of Chemistry, Graduate School of Science, Osaka University, Toyonaka, Osaka 560-0043, Japan

[2]Materials Sciences Research Center, Japan Atomic Energy Agency, Sayo-gun, Hyogo 679-5148, Japan

[3]Department of Applied Physics, Osaka University, Suita, Osaka 565-0871, Japan

[4]Institute of Radiation Sciences, Osaka University, Toyonaka, Osaka 560-0043, Japan

Abstract

To study the elementary steps in the Rochow-Müller process, we bombarded Cu(111) and Cu(410) with 0.7-1.9 eV supersonic molecular beams (SSMB) of CH_3Cl. We then identified the corresponding adsorbed species using X-ray photoemission spectroscopy (XPS) in conjunction with synchrotron radiation (SR). We found Cl as the dominant adsorbed species (much higher than that of adsorbed carbonaceous species) coming from the dissociative scattering of CH_3Cl. We also found that the threshold kinetic energy of the reaction depends on the crystal surface orientation.

1. Introduction

The Rochow-Müller process can be considered as one of the most important industrial processes. Its discovery in 1945 served as an important breakthrough in the production of silicone [1–4], allowing for high selectivity and simple procedures for industrialization. This so-called "direct synthesis" still stands as the most convenient and economical way to produce silicone monomers, and accounts for ca. 90% of starting materials for silicone production [4].

The Rochow-Müller process involves copper-catalyzed reactions[1–4], with dimethyldichlorosilane ($(CH_3)_2SiCl_2$, M2, the most desirable raw material for the silicone industry) as the main product. This makes the Rochow-Müller process a complicated many-body system, i.e., involving heterogenous (gas-solid) reaction with a solid catalyst. Despite experimental and theoretical efforts [3–12], a clear understanding of the underlying catalytic mechanism has remained elusive and, at times, even contentious [5]. One possible simplification of such a complex reaction would be to consider the interaction of CH_3Cl with pure Cu and Si surfaces [13–21].

Here, we report on how energetic CH_3Cl molecules react with Cu (111) and Cu(410). We bombarded the copper surfaces with 0.7~1.9 eV supersonic molecular beam (SSMB) of CH_3Cl. We then characterized the corresponding surfaces (identified the corresponding adsorbed species) using X-ray photoemission spectroscopy (XPS) in conjunction with synchrotron radiation (SR). We found Cl as the dominant adsorbed species (much higher than that of the adsorbed carbonaceous species) coming from the dissociative scattering of CH_3Cl. We also found that the threshold kinetic energy of the reaction depends on the crystal surface orientation.

2. Experimental Methodology

We performed all experiments with the surface reaction analysis apparatus (SUREAC 2000) built at BL23SU in SPring-8 [22,23]. Briefly, our surface reaction analysis chamber has a base pressure of $< 2 \times 10^{-8}$ Pa, and an electron energy analyzer (OMICRON EA125-5MCD). It also has a quadrupole mass spectrometer for monitoring the molecular beam, located opposite the SSMB CH_3Cl source.

We first cleaned the Cu(111) and Cu(410) samples by repeated sputtering with 1.5 keV Ar^+ and 30 min annealing at 723 ~ 773 K, until we can no longer detect impurities by synchrotron radiation XPS (SR-XPS). We generated 0.7 ~ 1.9 eV SSMB CH_3Cl via adiabatic expansion of a CH_3Cl and He gas mixture through a nozzle with a small orifice at nozzle temperatures T_N = 300 ~ 773 K. Mass fragment analyses of the beam profile indicate that no significant CH_3Cl dissociation occurs at these nozzle temperatures (cf.,

Supplementary Data 1). We irradiate the clean Cu surfaces with SSMBs of varying incident kinetic energies. We then perform SR-XPS measurements at 300 K using photon energy of ~711 eV. Our beam line at BL23SU is particularly suited for photon energies above ~500 eV. The photon energy allows for C-1*s* and Cl-2*p* spectra measurements with reasonably high S/N ratios (high photoionization cross sections) and without any secondary-electron background and various Auger peaks. The high-intensity focused X-ray beam also enabled us to measure the high-resolution XPS spectra in a short time with high S/N ratios, and to perform fine-peak deconvolution. We calculated the area intensities by subtracting the C-1*s* and Cl-2*p* background spectra measured by SR-XPS using the Shirley method [24].

3. Results and Discussions

3.1 Dominant Cl Adsorption Species (as compared to adsorbed carbonaceous species)

Figs. 1(a) and (b) show the Cl-2*p* and C-1*s* SR-XPS spectra taken after 1.9 eV CH_3Cl SSMB irradiation on Cu(111) and Cu(410), respectively, at surface temperature T_S = 300 K. The Cl-2*p* intensity peak has two components, viz., Cl-2$p_{1/2}$ and Cl-2$p_{3/2}$, due to spin-orbit interactions, with an energy difference of 1.6 eV on both surfaces. On Cu(111), the Cl-2$p_{3/2}$ intensity peak at 198.38 eV becomes noticeable ca. @0.002 ML Cl coverage, and grows with increasing CH_3Cl SSMB dose at nearly the same position (ca. 198.28 eV) @0.146 ML Cl coverage. (1 monolayer [ML] is ca. equivalent to one adsorbed atom per substrate Cu atom.) Similarly, on Cu(410), the Cl-2$p_{3/2}$ intensity peak at 198.54 eV becomes noticeable ca. @0.008 ML Cl coverage, and grows with increasing CH_3Cl SSMB dose at nearly the same position (ca. 198.44 eV) @ 0.238 ML Cl coverage. The negligible energy difference between the two Cl-*2p* intensity peak components and in Cl-2$p_{3/2}$ intensity peak energies for varying Cl coverages suggest very weak interaction between adsorbed Cl atoms, as if indicating isolated Cl atoms. On the other hand, compared to the Cl-2*p* intensity peaks, the C-1*s* intensity peaks remain negligible and broad, even at the highest attainable CH_3Cl SSMB dose on both surfaces

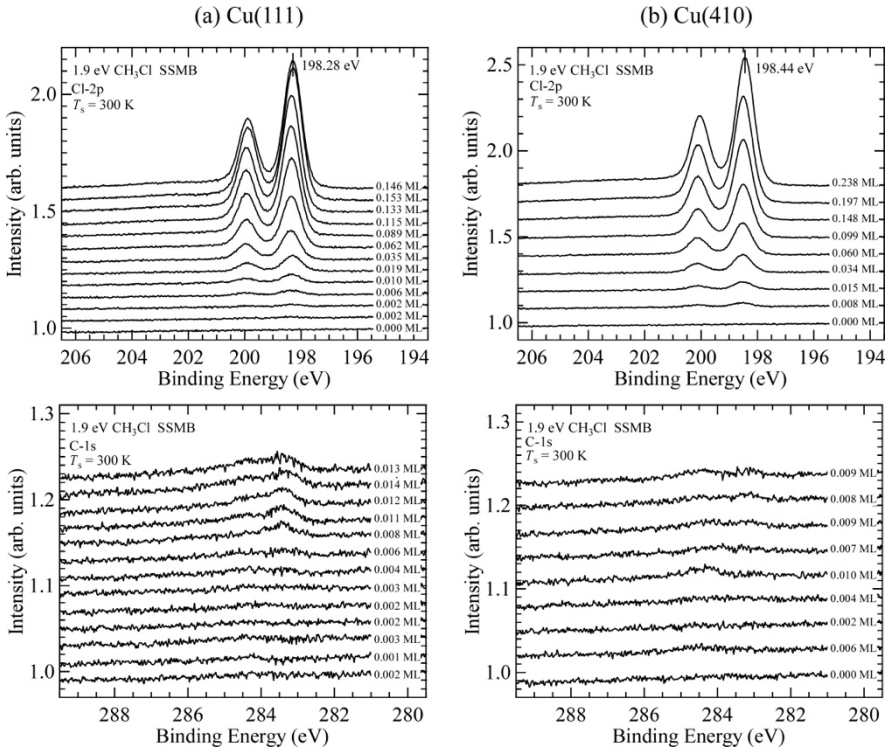

Fig.1 Cl-2*p* (upper panels) and C-1*s* (lower panels) XPS spectra and corresponding measured Cl coverages (in ML units, ca. equivalent to one adsorbed atom per substrate Cu atom), taken after 1.9 eV CH_3Cl SSMB irradiation on (a) Cu(111) and (b) Cu(410) at surface temperature T_S = 300 K, with a CH_3Cl flux density of 6.4×10^{14} molecules cm^{-2} sec^{-1}. The photoelectron detection angle $\theta = 0°$ (measured from the surface normal).

(cf., 283.40 and 284.46 eV on Cu(111) and 283.12 and 284.50 eV on Cu(410)). Note that we calibrated the C coverage using the C-1*s* XPS data taken from graphene grown on Cu(111) [25,26]. Similarly, we calibrated the Cl coverage based on the C-1*s* XPS data from graphene, by taking the photo-ionization cross section and the energy analyzer parameters, e.g., the photo-electron pass energy, into consideration [26]. The negligible and broad C-1*s* XPS intensity peaks on on both Cu surfaces indicate low coverage coming from carbonaceous species, viz., CH_3 and its dissociated species, e.g., CH_2.

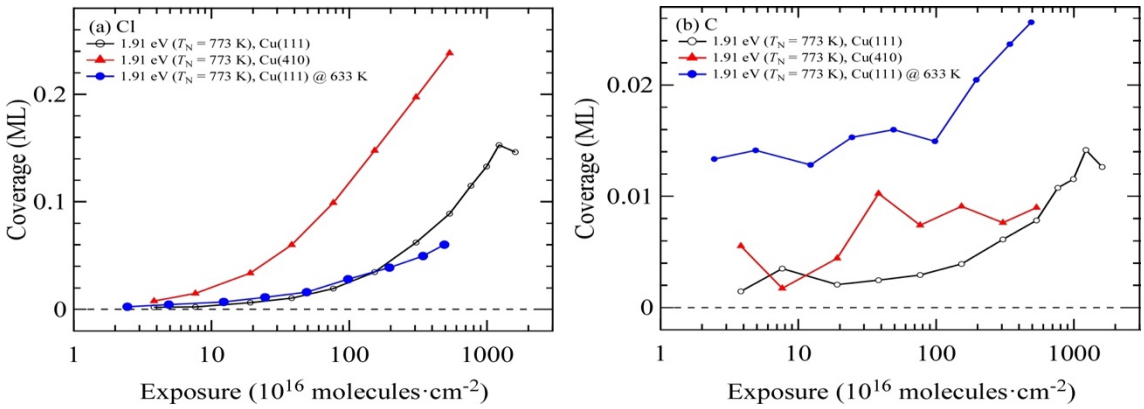

Fig. 2. (a) Cl and (b) C uptake curves produced by integrating a series of Cl-2*p* and C-1*s* XPS spectra on Cu(111) and Cu(410) surfaces, measured after 1.9 eV CH_3Cl SSMB irradiation at surface temperature T_S=300 K (on Cu(111) and Cu(410)) and T_S=663 K (on Cu(111)).

3.2 More Open Surface Preferred; Comparable Adsorption of Cl and Carbonaceous Species at Elevated T_S (> 300 K).

In Fig. 2, we show the uptake curves for (a) Cl and (b) C on Cu(111) and Cu(410), produced by integrating a series of Cl-2*p* and C-1*s* XPS spectra (see Fig. 1), measured after 1.9 eV CH_3Cl SSMB irradiation at T_S = 300 K (on Cu(111) and Cu(410)) and T_S = 663 K (on Cu(111)). From Fig. 1, we can estimate that Cl has 10 times higher coverage as compared to C-species (carbonaceous species) coverage, regardless of CH_3Cl SSMB dose. Previous studies (cf., e.g., [27]) indicate that, starting from (molecularly adsorbed) CH_3Cl, dissociative adsorption proceeds with both CH_3 and Cl adsorbed on Cu surfaces (Cl more stable than CH_3), and further CH_3 dissociation relatively unfavorable. Present results indicate that, instead of observing (the expected) equal adsorption of Cl and carbonaceous species (viz., CH_3), CH_3 could be scattered from the surface (instead of being adsorbed), leaving only adsorbed Cl on the Cu surfaces (*vide infra*). This could account for the difference in the corresponding C-1*s* and Cl-2*p* intensity peaks, as compared to that observed on Si(111) (i.e., comparable C-1*s* and Cl-2*p* intensity peaks, cf., e.g., Supplementary Data 2: Fig. 2S).

From Fig. 2, we can observe the following:

(1) The more open the surface, the more reactive it is to 1.9 eV CH_3Cl irradiation, and the presence of steps have negligible effect on reactivity. In order of decreasing reactivity we find Cu(410) ≈ Cu(100) > Cu(111) (cf., Supplementary Data 3: Fig. 3S).

Previous studies [27] report that, in order of decreasing Cl adsorption energy: Cu(410) > Cu(100) > Cu(111) > 3 eV. This indicates that once adsorbed at report T_S=300K, it may be difficult to desorb Cl. The trend in reactivity we observed here suggests the same conclusion with regard to Cl desorption.

(2) On Cu(111), at low exposures, we find similar Cl uptake curves (ca. same Cl coverage) for surface temperatures T_S = 300 K and 663 K. This continues with increasing exposure, and then the Cl coverage at T_S = 663 K becomes smaller than that at T_S = 300 K, with further increase in exposure. This may be due to Cl desorption as Cl_2 and/or CH_3Cl, as the adsorption energy decreases with increasing repulsive dipole-dipole interaction between the Cl adsorbates. (Note that the experimentally determined Cl diffusion barrier on Cu(111) is 0.2 eV [28].)

(3) On the other hand, also on Cu(111), we find higher C (carbonaceous species) coverage at T_S = 663 K as compared to that at T_S = 300 K. This may be due to further dehydrogenation of adsorbed CH_3 at elevated T_S.

(4) Thus, for Cu(111), at elevated T_S (T_S > 300 K, viz., T_S = 663 K), we observe comparable C (carbonaceous species) and Cl uptake curves on the surface.

3.3 Incidence Energy Dependence and Reaction Threshold (Kinetic) Energy

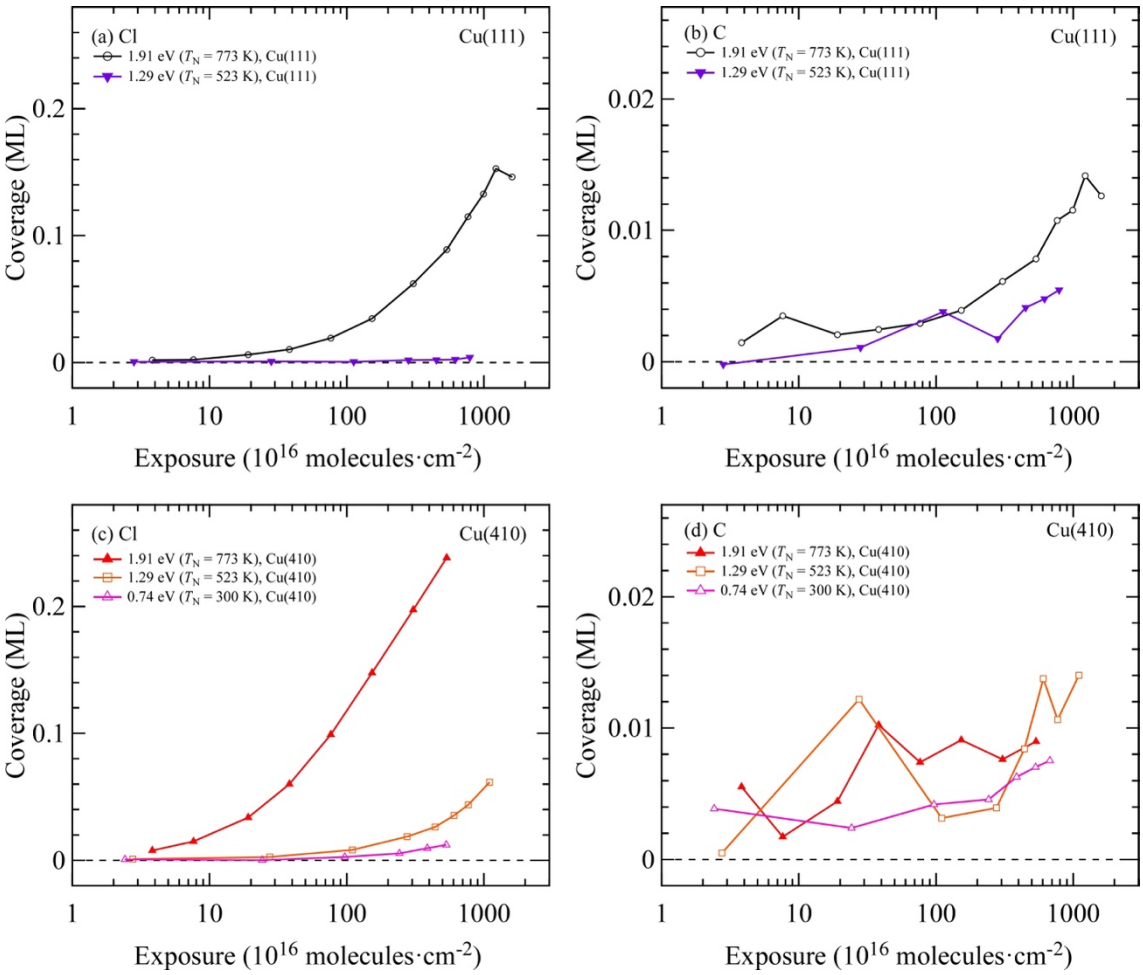

Fig. 3 Cl and C uptake curves produced by integrating a series of Cl-2*p* and C-1*s* XPS spectra on Cu(111) ((a) and (b), respectively) and Cu(410) ((c) and (d), respectively), measured after for 0.7, 1.3, and 1.9 eV (produced with nozzle temperatures T_N = 300, 523, and 773 K, respectively) CH_3Cl SSMB irradiation at surface temperature T_S = 300 K.

In Fig. 3, we show the incident energy dependent (a) Cl and (b) C uptake curves on Cu(111) and Cu(410), measured after CH_3Cl SSMB irradiation at T_S=300 K. The Cl uptake (indicating CH_3Cl dissociation) increases with increasing incident energy (viz., 0.74 eV, 1.29 eV, and 1.91 eV) on both surfaces, while the C uptake does not show any

clear incident energy dependence. Note the abstractive reaction of CH_3Cl needs to overcome some activation barrier along the reaction coordinate with CH_3 escaping the surface (reaction threshold energy, *vide infra*).

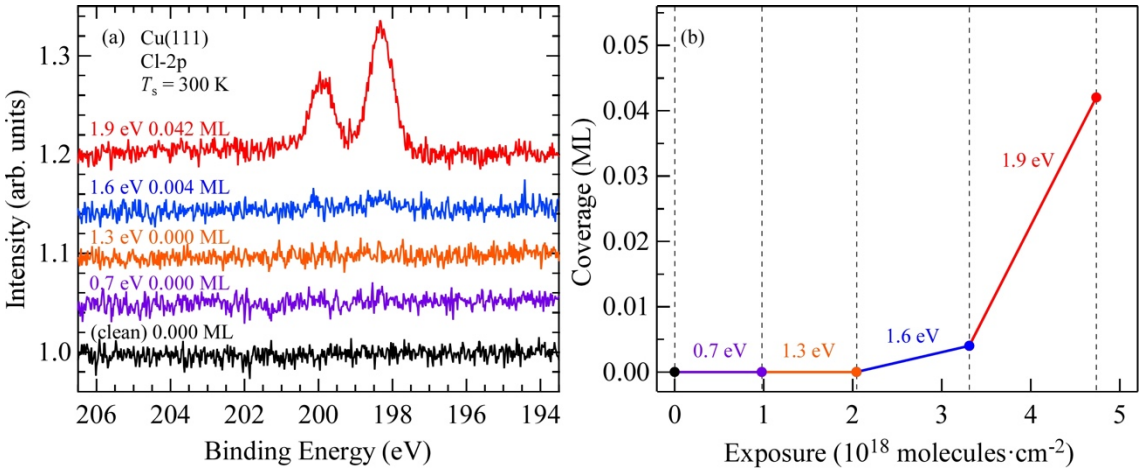

Fig 4. (a) Cl-2*p* XPS spectra on Cu(111), taken after CH_3Cl SSMB irradiation at T_S = 300 K, for various incident energies, and corresponding Cl coverage. Photoelectron detection angle θ= 0° (from the surface normal). (b) Cl uptake curve produced by integrating a series of Cl-2*p* spectra. At each kinetic energy step of the CH_3Cl SSMB, we continuously irradiate the surface without cleaning and measured the Cl coverage. We then increase the kinetic energy of the CH_3Cl SSMB and then repeat this irradiation-and-measuring cycle.

To clarify the incident-energy dependence of the reactivity and obtain its threshold, we measured the Cl coverage after dosing a certain amount of CH_3Cl (~1×10^{18} molecules cm^{-2}) at each kinetic energy step. At each kinetic energy step of the CH_3Cl SSMB, we continued to irradiate the surface without cleaning and measured the Cl coverage. We then repeated this irradiation-and-measuring cycle at the next kinetic energy step. Fig. 4 shows the incident energy dependence of Cl uptake and the corresponding Cl-2*p* XPS spectra on Cu(111). For Cu(111), we estimate a reaction threshold (kinetic) energy of ca. 1.6 eV. For Cu(410), we estimate a threshold energy of ca. 1.1 eV (cf., Supplementary Data 4: Fig. 4S). Previous studies found only molecularly adsorbed CH_3Cl on Cu(410) [20] and Ag(111) [21], at ca. 100 K. The adsorbed CH_3Cl desorbs from Cu(410) [20] and Ag(111) [21] at ca. 200 K and ca. 140 K, respectively. Thus, we could expect a rather high activation energy for the dissociative adsorption of CH_3Cl. Previous theoretical studies [27] report a threshold energy 0.99 and 0.81 eV for Cu(111) and

Cu(410), respectively. The slightly higher threshold energy in experiments may be due to the excitation of rotational motions of CH_3Cl in the high-temperature nozzle.

3.4 Reaction Mechanism

Next, we consider the reaction mechanism behind the experimental results obtained (*vide supra*):

(1) Dominant Cl adsorption (and likely scattering of the dissociated CH_3).
(2) Surface orientation dependence of the reaction (more open surface preferable).
(3) High reaction threshold kinetic energy.

The first observation, i.e., the dominant adsorption of Cl atoms on the surface may not be explained by the selective desorption of CH_3 after dissociative adsorption [27], because the (carbonaceous species) C coverage slightly increases with increasing T_S, as shown in Fig. 2(b).

As CH_3Cl approaches the metal (copper) surface, due to the image potential and the chemical interaction between the metal surface and CH_3Cl, the CH_3Cl affinity level drops down (towards the metal Fermi level E_F and away from the vacuum level). How deep the affinity level drop goes depends on the classical turning point of the collision [29], which in turn depends on the kinetic energy of CH_3Cl. When the affinity level drops below the metal (copper) surface E_F, electrons from the metal (copper) surface may transfer to the unoccupied dissociative (antibonding) state of CH_3Cl, resulting in the dissociation to Cl and CH_3: $e^- + CH_3Cl \rightarrow Cl^- + CH_3$ (Supplementary Data 5: Fig. 5S). Considering steric effects [14–21,30,31], i.e., preference for Cl-end collision rather than CH_3-end collision, Cl remains adsorbed on the surface with the remain energy from the dissociation carried away by CH_3.

The second and third observations can be understood by as follows. As noted earlier, this reaction depends both on the CH_3Cl kinetic energy and the metal (copper) surface work function W. Thus, one would expect this would be more likely observed with higher kinetic energies and smaller work functions. Consider for example Cu(111) and Cu(100), with work functions ca. 4.94 eV and 4.59 eV, respectively (i.e., $W_{Cu(111)} > W_{Cu(100)}$) [32,33]. We can also expect Cu(410) to have a smaller work function compared to Cu(100), i.e., $W_{Cu(110)} > W_{Cu(410)}$ [34]. This would explain the observed lower threshold energy observed for Cu(410) as compared to Cu(111). The lower reactivity of Cu(111) can be understood in terms of the surface orientation dependent binding energy of Cl (CH_3Cl) with the metal surface, and the corresponding charge transfer between the metal surface to impinging CH_3Cl

Also note that typical Rochow-Müller reactions operated at ~350 °C, where we could expect high surface diffusion of adatoms and CH_3Cl with high kinetic energies. Cu can supply the surface Cl atoms and gas phase CH_3. Also note that Si can adsorb both species [13,35] (See also Fig. 2S). Previous studies suggest Cu_3Si alloys as reaction centers of the Rochow-Müller process, where Cu_3Si may mix up the supplied Cl and CH_3 and then, proceed to M2 production [12]. The reactions on Cu_3Si induced by the energetic CH_3Cl would be an interesting subject for the forthcoming studies.

4. Summary

We bombarded Cu(111) and Cu(410) with a 0.7~1.9 eV CH_3Cl SSMB, and characterized the corresponding reacted surfaces using XPS in conjunction with synchrotron radiation (SR). We found the dominant adsorbed species are Cl atoms resulting from the abstractive dissociative adsorption of CH_3Cl. It is not expected from the dissociative adsorption ratio of [Cl] : [CH_3]=1 : 1. The threshold of the kinetic energy of CH_3Cl for this abstractive reaction depends on the crystal face. The Cu(111) with larger work function is less reactive in this mechanism. The charge transfer from the surface to CH_3Cl is a possible origin for the abstractive reaction. In the Rochow-Müller process, Cu may supply the surface Cl atoms and CH_3 radicals in the gas phase. As a result, both produced at high T_S will react with the nearby Si atoms.

Acknowledgements

The authors thank MEXT (Ministry of Education, Culture, Sports, Science and Technology-Japan) for Grants-in-Aid for Scientific Research (JP20K21171, JP15KT0062, JP26248006, JP20H02638). They are also thankful for the assistance by Yauka Hashimoto, Tetsuya Sakamoto, Naoyuki Shimode, Shizuka Nishi, Hikaru Yoshida, and all of the staff at BL23SU in SPring-8. The synchrotron radiation experiments were performed at BL23SU in SPring-8, with the approval of the Japan Synchrotron Radiation Research Institute (JASRI) and Japan Atomic Energy Agency (JAEA) (Proposal Nos. 2022B3801, 2022A3801, 2021B3801, 2021A3801, 2020B3801, 2020A3801, 2019B3801, 2019A3831, 2019A3801, 2018B3831, 2018B3801, 2018A3831, 2018A3801, 2017B3801, 2017A3801). This work was performed under the Shared Use Program of JAEA Facilities (Proposal Nos. 2019A-E13, 2018B-E12, 2018A-E17) with the approval of Nanotechnology Platform project supported by MEXT.

REFERENCES

[1] E.G. Rochow, The Direct Synthesis of Organosilicon Compounds, J. Am. Chem. Soc. 67 (1945) 963–965. https://doi.org/10.1021/ja01222a026.

[2] R. Müller, Über Silicone (I), Z. Angew., Chem. Silicone (Synth.). Chem. Tech. 2 (1950) 41–50.

[3] D. Seyferth, Dimethyldichlorosilane and the Direct Synthesis of Methylchlorosilanes. The Key to the Silicones Industry, Organometallics. 20 (2001) 4978–4992. https://doi.org/10.1021/om0109051.

[4] Y. Zhang, J. Li, H. Liu, Y. Ji, Z. Zhong, F. Su, Recent Advances in Rochow-Müller Process Research: Driving to Molecular Catalysis and to A More Sustainable Silicone Industry, ChemCatChem. 11 (2019) 2757−2779. https://doi.org/10.1002/cctc.201900385.

[5] K.M. Lewis, D.G. Rethwisch, eds., Catalyzed Direct Reactions of Silicon, Elsevier Science, London, England, 1993.

[6] J. Li, L.-L. Yin, Y. Ji, H. Liu, Y. Zhang, X.-Q. Gong, Z. Zhong, F. Su, Impact of the Cu_2O microcrystal planes on active phase formation in the Rochow reaction and an experimental and theoretical understanding of the reaction mechanism, J. Catal. 361 (2018) 73–83. https://doi.org/10.1016/j.jcat.2018.02.010.

[7] T.C. Frank, J.L. Falconer, Silane Formation on Silicon: Reaction Kinetics and Surface Analysis, Langmuir. 1 (1985) 104–110. https://doi.org/10.1021/la00061a017.

[8] K.A. Magrini, S.C. Gebhard, B.E. Koel, J.L. Falconer, Methyl chloride and trichlorosilane adsorption on Cu(110), Surf. Sci. 248 (1991) 93–103. https://doi.org/10.1016/0039-6028(91)90064-y.

[9] J.Y. Lee, S. Kim, Adsorption mechanism of CH_3Cl on Si(100)-2×1, Surf. Sci. 482–485 (2001) 196–200. https://doi.org/10.1016/s0039-6028(00)01018-9.

[10] K.A. Magrini, J.L. Falconer, B.E. Koel, ChemInform abstract: Direct Formation of $(CH_3)_2HSiCl$ from Silicon and CH_3Cl, ChemInform. 20 (1989). https://doi.org/10.1002/chin.198941220.

[11] T. Frank, Surface Analysis of Methylchlorosilane Formation Catalysis, J. Catal. 95 (1985) 396–405. https://doi.org/10.1016/0021-9517(85)90117-4.

[12] D.-H. Sun, B.E. Bent, A.P. Wright, B.M. Naasz, Chemistry of the direct synthesis of methylchlorosilanes from methyl + chlorine monolayers on a Cu_3Si surface, Catal. Letters. 46 (1997) 127–132. https://doi.org/10.1023/A:1019025325414.

[13] A. Woelke, S. Imanaka, S. Watanabe, S. Goto, M. Hashinokuchi, M. Okada, T. Kasai, Dissociative adsorption of methyl chloride on Si(001) studied by scanning tunneling microscopy, J. Electron Microsc. (Tokyo). 54 Suppl 1 (2005) i21-4. https://doi.org/10.1093/jmicro/54.suppl_1.i21.

[14] M. Okada, S. Goto, T. Kasai, Dynamical steric effect in the decomposition of methyl chloride

on a silicon surface, Phys. Rev. Lett. 95 (2005) 176103. https://doi.org/10.1103/PhysRevLett.95.176103.

[15] M. Okada, S. Goto, T. Kasai, Reaction-path selection with molecular orientation of CH_3Cl on Si{100}, J. Am. Chem. Soc. 129 (2007) 10052–10053. https://doi.org/10.1021/ja070931b.

[16] M. Okada, S. Goto, T. Kasai, Steric effects in dissociative adsorption of low-energy CH_3Cl on Si(100): Orientation and steering effects, J. Phys. Chem. C Nanomater. Interfaces. 112 (2008) 19612–19615. https://doi.org/10.1021/jp807052s.

[17] H. Ito, M. Okada, D. Yamazaki, T. Kasai, Steric effects in the scattering of oriented CH_3Cl molecular beam from a Si(111) surface, J. Phys. Chem. A. 114 (2010) 3080–3086. https://doi.org/10.1021/jp907225b.

[18] M. Okada, Surface chemical reactions induced by well-controlled molecular beams: translational energy and molecular orientation control, J. Phys. Condens. Matter. 22 (2010) 263003. https://doi.org/10.1088/0953-8984/22/26/263003.

[19] M. Okada, Supersonic molecular beam experiments on surface chemical reactions, Chem. Rec. 14 (2014) 775–790. https://doi.org/10.1002/tcr.201402003.

[20] T. Makino, S. Zulaehah, J.S. Gueriba, W.A. Diño, M. Okada, CH_3Cl/Cu(410): Interaction and Adsorption Geometry, J. Phys. Chem. C. 122 (2018) 11825–11831. https://doi.org/10.1021/acs.jpcc.8b01296.

[21] K. Takeyasu, M. Okada, Adsorption geometry of methyl chloride weakly interacting with Ag(111), J. Phys. Commun. 2 (2018) 075017. https://doi.org/10.1088/2399-6528/aad1d0.

[22] M. Okada, Y. Tsuda, K. Oka, K. Kojima, W.A. Diño, A. Yoshigoe, H. Kasai, Experimental and Theoretical Studies on Oxidation of Cu-Au Alloy Surfaces: Effect of Bulk Au Concentration, Sci. Rep. 6 (2016) 31101. https://doi.org/10.1038/srep31101.

[23] Y. Tsuda, J.S. Gueriba, T. Makino, W.A. Diño, A. Yoshigoe, M. Okada, Interface atom mobility and charge transfer effects on CuO and Cu_2O formation on $Cu_3Pd(111)$ and $Cu_3Pt(111)$, Sci. Rep. 11 (2021) 3906. https://doi.org/10.1038/s41598-021-82180-w.

[24] D.A. Shirley, High-Resolution X-Ray Photoemission Spectrum of the Valence Bands of Gold, Phys. Rev. 5 (1972) 4709–4714. https://doi.org/10.1103/physrevb.5.4709.

[25] S. Ogawa, T. Yamada, S. Ishidzuka, A. Yoshigoe, M. Hasegawa, Y. Teraoka, Y. Takakuwa, Graphene growth and carbon diffusion process during vacuum heating on Cu(111)/Al_2O_3 substrates, Jpn. J. Appl. Phys. (2008). 52 (2013) 110122. https://doi.org/10.7567/jjap.52.110122.

[26] In private communications with Ogawa and Takakuwa, we obtained the data on intensity ratio of C(1s)/Cu(3s) vs C coverage on Cu(111), measured in the same apparatus as we used. Then, we can calibrate our data of C1s in Cu(111) measured at the same photon energy and energy-analyzer parameters. From the intensity ratio of C(1s)/Cu(3s) vs C coverage on Cu(111), we also estimated Cl coverage using Cl(2p) after taking the photo-ionization cross section and the

energy analyzer parameters, e.g. the photo-electron pass energy, into considerations.

[27] I.-H. Svenum, S. Gouttebroze, F.L. Bleken, Toward Understanding the Formation of Coke during the MCS Reaction: A Theoretical Approach, J. Phys. Chem. C. 127 (2023) 6680–6689. https://doi.org/10.1021/acs.jpcc.2c08299.

[28] W.K. Walter, D.E. Manolopoulos, R.G. Jones, Chlorine adsorption and diffusion on Cu(111), Surf. Sci. 348 (1996) 115–132. https://doi.org/10.1016/0039-6028(95)00996-5.

[29] S. Holloway, J.W. Gadzuk, Charge transfer, vibrational excitation, and dissociative adsorption in molecule–surface collisions: Classical trajectory theory, J. Chem. Phys. 82 (1985) 5203–5215. https://doi.org/10.1063/1.448645.

[30] T. Fukuyama, M. Okada, T. Kasai, Steric effects in the scattering of oriented CH_3Cl molecular beam from a graphite surface: weak interaction of physisorption, J. Phys. Chem. A. 113 (2009) 14749–14754. https://doi.org/10.1021/jp904893z.

[31] I.V. Ionova, S.I. Ionov, R.B. Bernstein, An image charge model for the classical trajectory simulations of molecule-surface scattering: steric effects in the scattering of trifluoromethane on graphite (0001), J. Phys. Chem. 95 (1991) 8371–8376. https://doi.org/10.1021/j100174a060.

[32] J.F. Jia, Y. Hasegawa, K. Inoue, W.S. Yang, T. Sakurai, Steps on the Au/Cu(111) surface studied by local work function measurement with STM, Appl. Phys. A Mater. Sci. Process. 66 (1998) S1125–S1128. https://doi.org/10.1007/s003390051310.

[33] P.O. Gartland, S. Berge, B.J. Slagsvold, Photoelectric Work Function of a Copper Single Crystal for the (100), (110), (111), and (112) Faces, Phys. Rev. Lett. 28 (1972) 738–739. https://doi.org/10.1103/physrevlett.28.738.

[34] J. Wang, S.-Q. Wang, Surface Science Surface Energy and Work Function of Fcc and Bcc Crystals: Density Functional Study, Surf. Sci. 630 (2014) 216–224. https://doi.org/10.1016/j.susc.2014.08.017.

[35] T. Lim, J.C. Polanyi, H. Guo, W. Ji, Surface-mediated chain reaction through dissociative attachment, Nat. Chem. 3 (2011) 85–89. https://doi.org/10.1038/nchem.930.